

REVIEW • OPEN ACCESS

## Towards a free electron laser based on laser plasma accelerators

To cite this article: M E Couprie *et al* 2014 *J. Phys. B: At. Mol. Opt. Phys.* **47** 234001

View the [article online](#) for updates and enhancements.

You may also like

- [Relativistic effect in galaxy clustering](#)  
Jaiyul Yoo
- [Form factors in asymptotic safety: conceptual ideas and computational toolbox](#)  
Benjamin Knorr, Chris Ripken and Frank Saueressig
- [2020 roadmap on plasma accelerators](#)  
Félicie Albert, M E Couprie, Alexander Debus *et al.*

 **kiutra**

Easy-to-use and Helium-3 free  
cryogenics solutions

LEARN MORE

## Review

# Towards a free electron laser based on laser plasma accelerators

M E Couprie<sup>1</sup>, A Loulergue<sup>1</sup>, M Labat<sup>1</sup>, R Lehe<sup>2</sup> and V Malka<sup>2</sup><sup>1</sup>Synchrotron SOLEIL, L'Orme des Merisiers, Saint-Aubin, BP 48, 91192 Gif-sur-Yvette CEDEX, France<sup>2</sup>Laboratoire d'Optique Appliquée, ENSTA-ParisTech, CNRS, Ecole Polytechnique, UMR 7639, 91761 Palaiseau, FranceE-mail: [marie-emmanuelle.couprie@synchrotron-soleil.fr](mailto:marie-emmanuelle.couprie@synchrotron-soleil.fr)

Received 2 October 2014

Accepted for publication 15 October 2014

Published 24 November 2014

**Abstract**

The recent advances in developing compact laser plasma accelerators that deliver high quality electron beams in a more reliable way offer the possibility to consider their use in designing a compact free electron laser (FEL). Because of the particularity of these beams (especially concerning the divergence and the energy spread), specific electron beam handling is proposed in order to achieve FEL amplification.

Keywords: laser wakefield acceleration, free electron laser, seeding, undulator

**Introduction**

Third generation light provides tuneable light sources from infra-red to x-ray with a high average brightness [1] and high repetition rate. Without considering the solutions enabling us to shorten the bunch [2–4], the pulse duration stands in the picosecond range due to recirculation, and the peak power thus remains limited. Our quest is oriented towards shorter pulse duration and higher intensities for probing matter with greater temporal and spatial resolution. Presently, the highest peak intensities in the x-ray range are reached on fourth generation light sources, thanks to the free electron laser (FEL) process, enabling short pulses (femtosecond range), GW power, and longitudinal and transverse coherence.

Free electron lasers [5], as with conventional lasers, rely on the amplification of a light pulse in a gain medium, the medium being a relativistic electron bunch produced in an accelerator. For the amplification process to occur, the electron beam wiggles in the periodic magnetic field of an undulator under a resonance condition linking the beam energy to the undulator field period and strength. The light

pulse to be amplified can be either provided by the spontaneous synchrotron radiation of the beam in the undulator or by an external source. The gain of an FEL is strongly related to the electron beam quality, which is determined by its current, transverse size, divergence (i.e., emittance), charge, energy, and energy spread. The undulator [6] is characterized in terms of magnetic field period and strength—the higher the gain, the shorter the undulator length required to reach saturation, and the higher the beam quality, the higher the final output power.

FEL-based x-ray sources have already produced major breakthroughs because of their ability to study ultrafast phenomena in different domains of science [7]. The advent of these x-ray FELs also results from the high gains that are achievable, thanks to the development of radio frequency linear accelerators (LINACs), which now provide extremely good beam quality in terms of emittance, energy spread, and brightness. These facilities being in the km scale, new directions investigate how to make these FELs become more compact and more accessible to a larger number of users.

Using plasma acceleration fields of a hundred GV/m [8, 9], instead of the tens of MV/m in conventional RF ones, could enable the delivery of GeV electron beams within a few cm with a compact and high repetition rate laser system. This opens the possibility of a new class of compact FELs working at 10 Hz [10, 11]. Electron beams from plasmas have already



Content from this work may be used under the terms of the Creative Commons Attribution 3.0 licence. Any further distribution of this work must maintain attribution to the author(s) and the title of the work, journal citation and DOI.

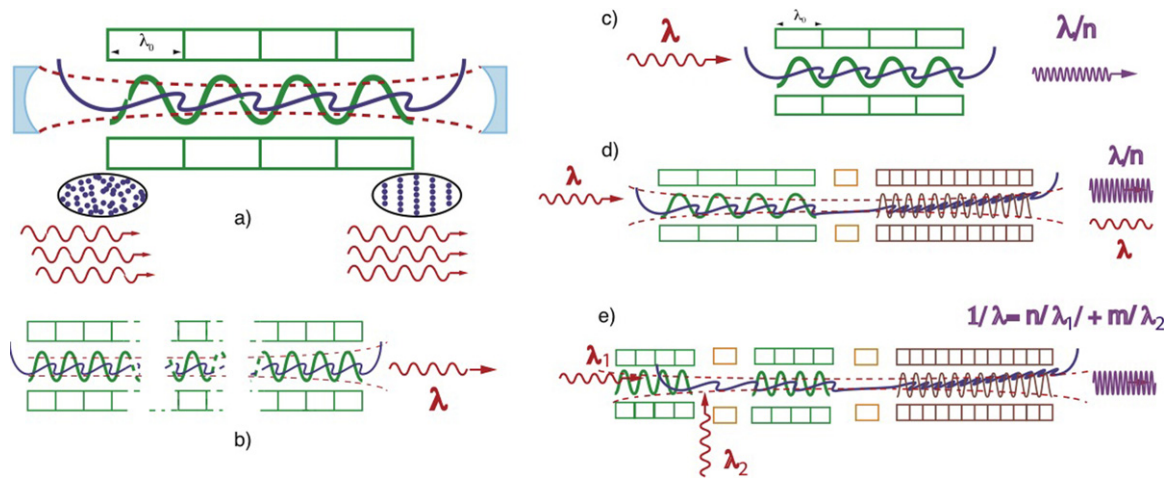


**Figure 1.** Free electron laser configurations: (a) oscillator case with an optical cavity enabling storage of the spontaneous emission; (b) self-amplified spontaneous emission (SASE), where the spontaneous emission emitted in the beginning of the undulator is amplified in one single pass; (c) seeding, where a coherent source tuned to the resonant wavelength of the undulator enables us to perform efficiently the energy exchange leading to the density modulation; (d) high gain harmonic generation; and (e) echo enabled harmonic generation (EEHG).

been successfully transported to an undulator and have produced spontaneous emissions [12–14]. But achieving FEL amplification remains to be demonstrated: the difficulty comes from the intrinsic properties of the electron beam. Indeed, for an energy of a few hundreds of MeV, while LINAC beams exhibit typically 1 mm transverse size, 1  $\mu$ rad divergence with 1 mm longitudinal size, and 0.01% energy spread, plasma beams are more likely 1  $\mu$ m transverse size, 1 mrad divergence with 1  $\mu$ m longitudinal size, and 1% energy spread.

We report here on the recent progress that will allow us, with realistic electron beam parameters that will be shortly produced by laser plasma accelerators, to demonstrate FEL amplification.

## 1. Free electron lasers

### 1.1. Free electron laser physics

The FEL was proposed in 1971 [5]. The FEL starts from the spontaneous emission, which is the synchrotron radiation generated by a relativistic electron beam wiggling in an undulator, creating a permanent periodic (period  $\lambda_u$ ) magnetic field  $B_u$ . Synchrotron radiation from an undulator source consists of a series of harmonics or order  $n$ , according to the so-called resonance condition:  $\lambda = \lambda_u(1 + K^2/2)/2n\gamma^2$  with the deflexion parameter  $K_u = 0.94\lambda_u$  (cm) $B_u$  (T) and  $\gamma$ , the normalized electron beam energy to its rest energy. The light wave of wavelength  $\lambda$  interacts with the electron bunch in the undulator, inducing an energy modulation of the electrons that is gradually transformed into density modulation at  $\lambda_u$ , enabling phased electrons to produce emission coherently at  $\lambda_u$  and its harmonics of order  $n$ . The light wave—electron interaction can lead to a light amplification to the detriment of the kinetic energy of the electrons. The small signal gain is proportional to the electronic density and varies as the inverse of the cube of the electron beam energy, depending on the

undulator length. Operation at short wavelengths requires high beam energies for reaching the resonant wavelength and thus long undulators (100 m–1 km for 1  $\text{\AA}$ ) and high electron beam density (small emittance and short bunches) for ensuring a sufficient gain. After the light amplification, the electron energy spread is enlarged, its average energy being reduced so that the gain decreases and/or the resonance condition is no longer fulfilled: the FEL saturates [15]. Besides, the light travels slightly faster than the electrons (it slips over one wavelength for one undulator period (slippage)), and the undulator is limited to a length that does not allow the light to substantially escape from the electron bunch distribution. The FEL wavelength is simply changed by modifying the magnetic field of the undulator in a given spectral range set by the electron beam energy. The polarization depends on the undulator configuration.

Various configurations are used (see figure 1). In the oscillator, the spontaneous emission is stored in an optical cavity, enabling multiple interactions between the electron beam and the light wave. An external laser can also be superimposed on the electron beam in the undulator that is tuned on the laser wavelength, and it allows for an efficient energy exchange and harmonic generation. The use of a coherent external source tuned on the undulator resonance wavelength is referred to as seeding in the high gain context. Because of the limited performance of mirrors, high gain short wavelength FELs are usually operated in the so-called self-amplified spontaneous emission (SASE) setup, where the spontaneous emission at the input of the FEL amplifier is amplified, typically up to saturation in a single pass after a regime of exponential growth. Once the saturation is reached, the amplification process is replaced by a cyclic energy exchange between the electrons and the radiated field.

So far, FELs have been installed on different types of accelerators [16]. Storage rings provide rather long electron bunches (10–30 ps) because of the electron beam recirculation. Linear accelerators provide a very short bunch of 10 fs–

10 ps duration, of interest for ultrashort pulse source production and for high electron beam densities. An energy recovery LINAC (ERL) combines advantages of both types, with short pulses, few recirculation turns, and energy recovery for power consumption savings. For LINAC-based FELs and ERL, RF photo-injectors are currently used.

### 1.2. Infrared to VUV FELs with FEL oscillators and coherent harmonic generation

The FEL was first experimentally demonstrated in 1977 in Stanford (USA) in the infrared, using the MARK-III linear accelerator [17] in the oscillator configuration on a superconducting linear accelerator. The second FEL in the visible range was then achieved in 1983 on a storage ring [18] in Orsay, France. Very quickly afterwards, the ultraviolet (UV) and VUV were reached with harmonic generation [19–21]. FEL oscillators in the UV have then been developed in different places such as VEPP3 [22], Super-ACO [23], Teras [24], NIJI-IV [25], UVSOR [26], DELTA [27], DUKE [28], and ELETTRA [29] on storage rings and on LINACs at FELI [30], Jefferson Lab [31], and Jaeri [32]. Oscillator-based FELs intrinsically present a very good transverse coherence, as it is mainly determined by the optical cavity [33].

The Super-ACO FEL was first employed for users in the UV [34] in association with synchrotron radiation for pump-probe two color experiments [35, 36]. The use of the gamma-ray generated by Compton backscattering has been extensively developed in the DUKE FEL [37]. Industrial applications of kW UV FELs have been developed at Jefferson Lab [38].

The record of the shortest FEL oscillator has been achieved on the ELETTRA storage ring at 193 nm [39]. Indeed, besides the value of the reflectivity in the specific spectral range, mirror degradation can occur because of the synchrotron radiation harmonic content hitting the optics [40–42].

### 1.3. Single-pass FEL in the x-ray range

The most usual configuration for an x-ray FEL is the SASE one [43–45]. The output power follows [46]:  $P(z) = P_0 \times \exp(z/L_g)$ , with  $P_0$  the initial synchrotron input power and  $L_g$  the gain length characterizing the efficiency of the amplification. Saturation is reached typically after  $20 \times L_g$  [47], and the power is orders of magnitude higher than the simple undulator spontaneous emission. Thanks to recent accelerator advances (high peak current, small energy spread, low emittance) and long undulator LINAC-based single-pass SASE, FELs are blooming worldwide. They now provide tunable coherent sub-ps pulses in the UV/x-ray region, with record peak powers (typically GW) and a substantial gain in peak and average brilliance. After LEULT (Argonne, USA) [48] SASE achievement in the VUV, FLASH I and II (Germany) (30–4.5 nm) [49, 50] operates for users, the SCSS Test Accelerator (Japan), (40–60 nm) [51] is presently upgraded after serving users. In the Angstrom (Å) region, the first tunable fs x-ray FEL has been achieved with 1.5 Å

(1–10 keV) wavelength and several mJ output energy at the Linear Coherent Light Source (LCLS, Stanford, USA) [52, 53] in 2009, using one part of the existing next linear collider test accelerator (SLAC) room-temperature LINAC at 14 GeV. LCLS II is under construction, with a superconducting LINAC and flexible polarization [54]. The Spring-8 Angstrom Compact free electron LAsER (SACLA), the second worldwide x-ray FEL extending the radiation down to 0.06 nm, has operated since June 2011 [55] (Japan, 8 GeV). SACLA (5–20 keV) operates with a thermo-ionic gun, a C band compact linear accelerator of 8 GeV, 18 five-meter long in-vacuum undulators of 18 mm period length with adjustable gaps. Fifty years after the laser discovery [56], these x-ray FELs constitute the brightest x-ray photon beams ever produced without competing conventional lasers. They have already successfully enabled various user applications, opening a new era for the investigation of matter [57–65], especially for pump/resonant x-ray probe experiments in combination with synchronized lasers or for imaging. This major breakthrough arises from the joint accelerator and FEL developments. Additional x-ray FEL facilities are forthcoming, such as the European XFEL [66] on a high repetition rate superconducting linear accelerator, the Korean XFEL [67], and the Swiss FEL [68]. The present trend is to provide a higher availability of the x-ray pulses with high repetition rate operation through the use of superconducting linear accelerators. These x-ray FELs, of a typical km length, typically use 100 m of undulators.

In the SASE regime, the emission usually presents poor longitudinal coherence properties, with temporally and spectrally spiky emissions resulting from non-correlated trains of pulses [69]. It is possible to suppress the spikes, to improve the longitudinal coherence, and to reduce the intensity fluctuations and the jitter when the FEL amplifier is seeded with an external coherent light source that possesses the required coherence properties [70]. The seed can be an external laser wave or a short wavelength coherent light source, such as high order harmonics generated in gas (HHG) [71, 72], which is injected in order to interact with the electron beam in the undulator. Saturation is also more rapidly reached than in the SASE case, which makes the system more compact. In the high gain harmonic generation scheme (HGHG) [73], a first laser tuned on the first undulator induces the modulation in density of the electron bunch, and the radiation is produced in the second undulator tuned on the harmonic of the injected wavelength. The FEL pulse temporal and spectral distributions result from the seed and the FEL intrinsic dynamics. In a variant, the so-called harmonic cascade configuration, the wavelength ratio of the two stages is a ratio of integers [74]. In particular cases, super-radiant modes exhibit further pulse duration narrowing and intensity increase [74]. HHG seeding was first performed on the SCSS Test Accelerator at 160 nm [75] and at 60 nm [76], at SPARC with cascading demonstration [77], and at 30 nm at s-FLASH [78]. The only seeded FEL users' facility is FERMI@ELLETRA (Trieste, Italy) [79], which uses a conventional laser as a seed. The combination of HGHG, the fresh bunch technique—where the light interacts in the second undulator in a non-heated part of the

electron bunch [80]—and harmonic cascade has recently enabled a frequency up conversion by a 192 factor [81]. FERMI equipped with APPLE-II undulators [82] also provides circular polarization to users. The seed level should overcome the shot-noise [83], and this can become critical for a short wavelength seed. Seeding enables us as well to get harmonics up-conversion to a higher order than in the SASE case [84].

Efficient up-frequency conversion can also be performed with two successive electron—laser interactions in two undulators in the EEHG [85] scheme, in imprinting a ‘sheet-like structure’ in phase space. A conceptual breakthrough in up-frequency conversion, it has been experimentally demonstrated first up to the seventh harmonic [86] and up to the fifteenth [87] on the SLAC and on the Shanghai FEL Test Facility [88]. Schemes derived from EEHG, such as the triple mode chicane [89], open perspectives for very short wavelength (Å) and short duration at moderate cost.

There are alternative solutions to handle the spiky spectral and temporal structure of the SASE besides seeding with laser and HHG. The simplest solution is to operate with low charge short electron bunches, providing a single spike regime [90] with a slightly reduced intensity, as was recently achieved at LCLS [91]. Alternatively, an electron beam energy chirp (electron energy dependence along the bunch position) combined with undulator taper (variation of the peak field along the longitudinal direction) can also efficiently lead to a single-spike FEL, as experimentally demonstrated at SPARC [92]. Proper combinations of chicanes and undulator segments can enable us to phase-lock the radiation [93] (e.g., improved SASE and purified SASE). In addition, after the proposal of seeding directly with the FEL [94], self-seeding emerged rapidly with the idea of using a single crystal monochromator [95] for the spectral selection, with the self-seeding operation both at LCLS [96] and at SACLA [97].

FELs generally present a good transverse coherence [98] and wavefront [99].

Following the first results achieved in the infrared on an oscillator [100, 101], single-pass FELs at short wavelength can also provide two simultaneous colors with adjustable delay. In the SASE case, with a sufficient margin of undulator length, two colors are generated in tuning the two series of undulators at different wavelengths with the delay adjusted by a chicane, such as the one that can be installed for self-seeding [102]. In the seeding case, one can fruitfully take advantage of the pulse splitting effect that can occur for a particular seed pulse duration with respect to the electron bunch length [103], as shown at FERMI@ELETTRA with a chirped seed [104].

One present trend in FEL development focuses on the improvement of performance in a wide spectral range, with versatile properties and flexibility for users. One aspect concerns the multiple user operation for reducing the operating cost per experiment. By enhancing the repetition rate of the accelerator, thanks to the superconducting technology, successive electron bunches or trains can be kicked toward different FEL lines, which then operate simultaneously [50, 105]. Additionally, with a proper setting of the phase of

the accelerating sections, bunches of various beam energies can be kicked to different FEL lines to enable a widening of the spectral range [106]. The other trend aims at reducing the size, either by exploring further seeding and/or by replacing the conventional linear accelerator with a compact alternative one. One can consider laser wakefield accelerators (LWFA) [9, 10], dielectric accelerators [107, 108], and inverse FELs [109, 110]. Combining a superconducting LINAC, an LWFA, and advanced seed schemes is also the key concept of the LUNEX5 (a free electron Laser Using a New accelerator for the Exploitation of x-ray radiation of 5th generation) demonstrator project [111, 112]. Indeed, it aims to investigate the production of short, intense, and coherent pulses in the soft x-ray region (4–40 nm). The LWFA will be qualified in view of FEL application. The single FEL line will be composed of the most advanced seeding configurations (HHG seeding and EEHG) and will be completed by pilot user experiments to characterize and evaluate performance of these sources from a user perspective.

## 2. Progress on laser plasma accelerators

Since the accelerating field in superconducting radio frequency cavities is limited to about  $100 \text{ MV m}^{-1}$ , the length of accelerators has to increase in order to achieve higher energy gain. To overcome this size issue, the use of an ionized medium (a plasma) that can sustain extreme electric fields naturally appears. The pioneering theoretical work performed in 1979 [8] showed how an intense laser pulse excites a wake of plasma oscillations through the non-linear ponderomotive force associated with the laser pulse. In this scheme, relativistic electrons were injected externally and were accelerated through the very high electric field sustained by relativistic plasma waves driven by lasers. The recent development of laser plasma wakefield accelerators [113, 114] opens a new path towards compact FELs. In this approach, an intense laser pulse can drive plasma density wakes to produce, by charge separation, strong longitudinal electric fields. The accelerating gradient could reach a few hundreds of GV/m [115]. Since then, plasmas have been recognized as a promising accelerating media. Thanks to the continuing efforts of the community, major breakthroughs have shown the possibility to produce stable and high quality electron beams with controllable parameters. Controlled injection is crucial for producing high quality electron beams. It is particularly challenging in laser plasma accelerators, because the length of the injected bunch has to be a fraction of the plasma wavelength, with typical values in the 10–100 microns range. In this case, electrons experience the same accelerating field, leading to the acceleration of a ‘monoenergetic’ and high quality bunch. Electrons can be injected if they are located at the appropriate phase of the wake and/or if they have sufficient initial kinetic energy. Different schemes (the colliding laser pulse scheme is shown on figure 2) have been demonstrated and allow for the control of the phase of injected electrons [116–126].

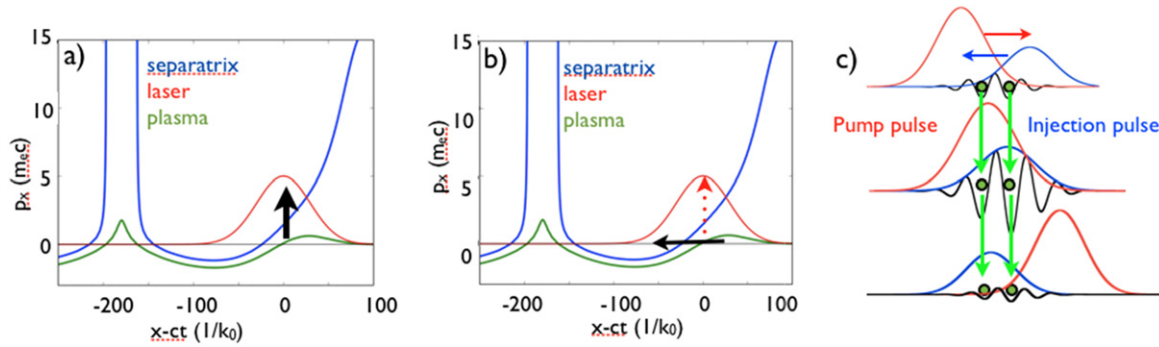


**Figure 2.** Principle of injection by colliding laser pulses: (a) in the ‘hot’ injection scheme, injection is achieved thanks to momentum (red) gained by electrons from the plasma wave (green) during the collision, which allows them to cross the separatrix (blue); (b) in the ‘cold’ injection scheme, electrons are injected by being dephased from the front of the main pulse to its back without momentum gain (black); (c) principle of electron dephasing in a standing wave (dotted line) generated by the collision between two counter-propagating circular laser pulses.

The recent demonstration of the colliding laser pulses scheme [116] (with a moderate laser energy—0.7 J laser energy for the pump laser and 0.2 J for the injection laser pulse) has allowed the production of a high quality electron beam with parameters that still need to be improved for the demonstration of FEL gain. With the increase of the laser energy (two laser beams of 2 J each), new injection schemes are proposed in order to reach the objective.

In 2006, stable and tunable ‘quasi-monoenergetic’ electron beams were measured by using two counter-propagating laser beams in the colliding pulse scheme [116]. The use of two laser beams instead of one offers more flexibility and enables one to separate the injection from the acceleration process. The first laser pulse (the pump pulse) is used to excite the wakefield, while the second pulse (the injection pulse) is used to heat electrons during its collision with the pump pulse. After the collision has occurred, electrons are trapped and further accelerated in the wakefield. As the overlapping of the lasers is short in time, the electrons are injected in a very short distance and can be accelerated to an almost ‘monoenergetic’ beam. This concept was validated in an experiment using two counter-propagating pulses. It was shown that the colliding pulse approach allows control of the electron beam energy, which is done simply by changing the delay between the two laser pulses and control of the charge and energy spread by changing the injection laser intensity, the electron density, or the relative polarization of the two laser pulses. The robustness of this scheme also permits us to carry out very accurate studies of the dynamics of the electric field in the presence of a high current electron beam. Indeed, in addition to the wakefield produced by the laser pulse, a high current electron beam can also drive its own wakefield. This beam loading effect was used to reduce the relative energy spread of the electron beam to the 1% level [127]. The existence of an optimal load was observed experimentally and supported by full three-dimensional particle-in-cell (PIC) simulations, and it corresponds to a peak current in the 20–40 kA range. To improve the electron beam quality, new ideas regarding injection control with two laser pulses, such

as the cold injection scheme or transverse colliding laser pulses scheme, will be addressed experimentally here.

### 2.1. Cold injection scheme

In the cold injection scheme [128], two laser pulses with circular polarization collide in the plasma and produce a standing wave that freezes electrons at the collision point, as shown in figure 2. After the collision, these electrons are accelerated in the plasma wakefield, driven by the pump beam. In this case, no heating is needed, and electrons cross the separatrix because they keep a constant longitudinal momentum.

With reasonable laser and plasma parameters, such as for the main laser pulse parameters  $a_0 = 4$ ,  $w_0 = 18 \mu\text{m}$ ,  $\tau_0 = 30 \text{ fs}$ , for counter-propagating laser pulse  $a_1 = 0.1$ ,  $w_1 = 15 \mu\text{m}$ ,  $\tau_1 = 30 \text{ fs}$  ( $w$  is the focal spot size, the index 0 and 1 refer, respectively, to the pump and to the injection laser pulses), and for the plasma, a density is constant at  $n_e = 2.5 \times 10^{-4} n_c$ . Simulations show that a 62 MeV beam could be produced with an energy spread of about 1% with a few tens of pC of charge. Therefore, the energy spread can still be improved by injecting a lower charge or by shaping temporally the injected electron bunch.

### 2.2. Transverse injection in colliding laser pulses scheme

Transverse injection with colliding laser pulses [129] is a new mechanism that we have observed in PIC simulations. This mechanism contrasts with previously observed optical injection mechanisms, which were essentially longitudinal. This transverse injection is caused by a transient expansion of the accelerating bubble, which is itself a consequence of the electron dynamics during the pulse collision. In this process, good-quality electron bunches (50 pC, 3% energy spread) having emittance lower than 0.15 mm.mrad should be produced. Simulations show that in a proper parameters regime, the bubble as a whole is strongly affected. This deformation is essential for injection. As shown below, right after the collision, the bubble transiently shrinks and re-expands, and this re-expansion triggers the injection of off-axis electrons.

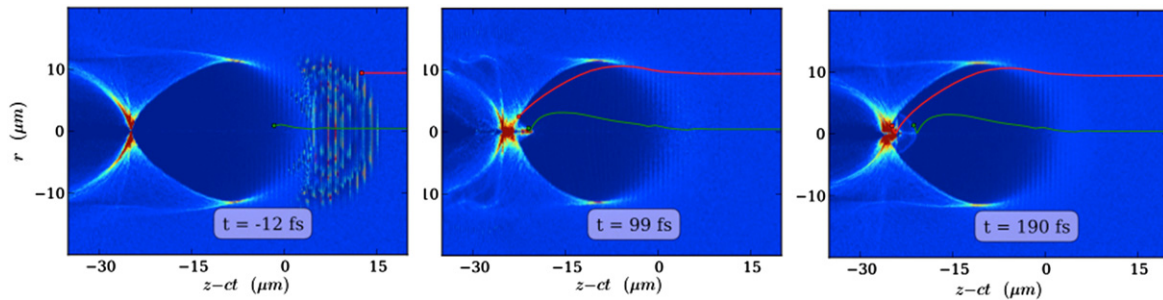


**Figure 3.** Snapshots of the electron density during the colliding pulse simulation. Labels indicate the time with respect to the moment of the collision. The red line represents the trajectory of a typical transversely injected electron in the moving window. The green line depicts the trajectory of an electron representative of cold injection.

Three consecutive snapshots of this simulation are shown in figure 3. As mentioned before, the bubble transiently shrinks (between  $t=70$  fs and  $t=100$  fs) and re-expands (between  $t=100$  fs and  $t=150$  fs), the rear of the bubble moving forth and then back. A first injected bunch with a low amount of charge (13 pC) is observed at  $t=99$  fs (i.e., before the bubble starts re-expanding) and at the position  $z-ct = -23 \mu\text{m}$ . It has all the characteristics of cold injection, and, in particular, it is composed of electrons that were initially near-axis, as can be seen from the green trajectory. A second bunch appears after the bubble expands at  $z-ct = -25 \mu\text{m}$ . It contains a much larger amount of charge (50 pC). As can be seen from the plotted trajectory, these electrons come from a large initial radius and arrive at the rear of the bubble exactly at the moment that it re-expands. No further injection occurs once the bubble stops expanding. All these features are consistent with the theory of injection in an evolving bubble [129]. The physical explanation for this phenomenon is that these electrons would normally slip out of the bubble if it were static, but since the bubble expands as they arrive at its rear, they remain a little longer inside it and are accelerated a little more, providing them enough speed to be injected. The bunch has a good quality: its duration is as short as 3 fs, and its absolute energy spread is 1 MeV (3% relative energy spread at 27 MeV). The most remarkable feature of this injection, and its main advantage over other optical injection methods, is its very low normalized transverse emittance. For the electrons from transverse injection, we obtained  $\epsilon_x \approx \epsilon_y < 0.15 \text{ mm.mrad}$ . By comparison, the emittance of the electrons from cold injection is 1.9 mm.mrad.

In consequence, LWFA can nowadays produce electron beams in the few hundreds of MeV to 1 GeV range [130–133] with a typical current of a few kA [134] with reasonable beam characteristics (relative energy spread of the order of 1% [127] and a normalized emittance of  $\sim \pi \text{ mm.mrad}$  [135–137].

### 3. Strategies towards LWFA-based FELs

Following the recent development of LWFA exposed in the previous section, one can here consider electron beams with a typical current of a few kA, bunch length of a few fs, energy in the few hundreds of MeV to 1 GeV range, electron

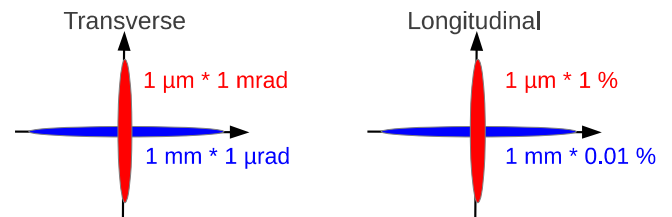


**Figure 4.** Simplified sketch of transverse (left) and longitudinal (right) phase space comparison between conventional LINAC (blue) and LWFA (red) beams.

divergence of typically 1 mrad, an energy spread of the order of 1%, and normalized emittance (product of transverse beam size and divergence) of the order of  $\pi \text{ mm.mrad}$  for studying the FEL amplification. For comparison, standard LINACs with gradients of a few tens of MV/m deliver for x-ray FEL beams 1 nC charge,  $1 \pi \text{ mm.mrad}$  emittance, and 0.01% energy spread at several GeV. LWFA has still a much larger energy spread. They so far enable us to observe undulator spontaneous emission [12–14]. Experiments aiming at achieving FEL amplification are under way in various places (LOASIS (Berkeley) [138, 139], Strathclyde University [140], MPQ [141], LOA /SOLEIL in the frame of the LUNEX5 project [142], *et al*).

However, using electron beams with the presently achieved performance in terms of energy spread and divergence does not lead to direct FEL amplification. Typically, more than one order of magnitude has to be gained in the energy spread value, the large divergence has to be handled, and daily operation should be more reliable for achieving proper FEL saturation. An adequate beam manipulation through the transport to the undulator is required for FEL amplification.

#### 3.1. LWFA electron beam properties

With respect to conventional accelerators, LWFA beams present very different characteristics of phase space: in longitudinal, short bunch duration, and large relative energy spread and in transverse, large divergence, and micrometer size. Indeed, LWFA beams somehow exhibit orthogonal characteristics as compared to conventional accelerators (see figure 4). With a typical divergence of 1 mrad, bunch lengthening induced by the slowed large diverging particles

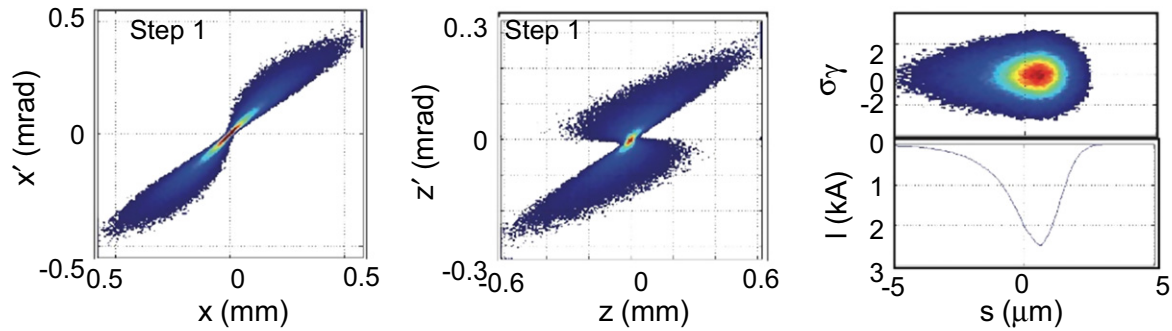


**Figure 5.** Transverse and longitudinal phase space calculated with tracking homemade simulation starting from a 400 MeV electron beam with 1 mm.mrad normalized emittances with a size of 1  $\mu\text{m}$  and a divergence of 1.25 mrad, a 1% energy spread for a 2 fs RMS pulse, and a 20 pC charge leading at the exit of the first step, with a triplet of 150 T  $\text{m}^{-1}$  located 5 cm from the source: 2.2 kA, 20 pC, large up to 20 (horizontal) and 70 (vertical) mm.mrad emittance with correlation with position, 1% slice energy spread.

can easily occur. In addition, there might also be an increase of the chromatic total emittance because of the large divergence. The initial short bunch (or high peak current) and emittance may then be rapidly spoiled.

### 3.2. Handling of the divergence

To preserve the emittance and the bunch length, the beam has to be refocused just after the gas cell of electron generation [143–146]. One assumes a six-dimensional (6D) Gaussian distribution without any correlations, analytical estimations that can be derived up to the second order, and a short duration low emittance electron bunch with large initial divergence propagation in free space. One considers a strong magnet quadrupole, located at a distance  $L_q$  from the source; its integrated normalized strength  $K_q$  has to equal  $1/L_q$  to cancel the divergence.

The RMS bunch length  $\sigma_s$  after the quadrupole is given by  $\sigma_s^2 = \sigma_{s0}^2 + 3\sigma_{x0}^4 L_q^2 / 2$ , and the total normalized emittance after the quadrupole  $\epsilon_n$  is expressed as  $\epsilon_n^2 = \epsilon_{n0}^2 + \sigma_{x0}^4 L_q^2 \sigma_{\gamma 0}^2$ , with  $L_q$  the quadrupole position from the source,  $\sigma_{s0}$ ,  $\sigma'_{x0}$ ,  $\sigma_{\gamma 0}$ , and  $\epsilon_{n0}$  the initial rms bunch length, divergence, energy spread, and normalized total emittance.

To limit the emittance and bunch duration growth, the quadrupole should be located as close as possible to the source, which implies the need to install very strong and compact quadrupoles [146]. This is illustrated in the case of the LUNEX5 parameters: a 6D Gaussian bunch without any correlations at 400 MeV, having a total normalized rms emittance of 1  $\pi$ .mm.rad (1 m 1.25 mrad), a 1% rms relative energy spread with an rms bunch length of 2 fs, and a moderate charge of 20 pC, leading to 4 kA peak current. The beam divergence induces second order bunch lengthening and an achromatic total emittance increase, leading to a butterfly-like transverse phase space, as shown in figure 5. These second order effects are contained for small values of  $L_q$ , i.e., in locating the quadrupole close to the source (here 5 cm), thus requiring a compact and very strong permanent triplet of quadrupole magnets of a few hundred T/m [147]. We found almost no amplification with 3D analytic expression of the FEL gain [148] and GENESIS [149] simulations, mainly because of the too-large value of the slice energy spread. The

slippage (difference in speed between electrons and emitted light ( $cK_u^2/4\gamma^2$ ), i.e.,  $N\lambda$ , with  $N$  the number of the undulator period) also limits the possible FEL amplification, since the light is rapidly escaping the electron bunch's longitudinal distribution (lasting only a few fs) after only few periods (six for 200 nm and 4 fs). At minimum, a reduction of the energy spread by a factor 10 down to 0.1% is mandatory to start the FEL process.

### 3.3. Handling of the energy spread

A spread in the average electron beam energies will lead to a spread of the resonant condition and degrade the FEL gain. There are different strategies for handling the energy spread.

The first one consists of implementing a chicane [150–152] composed of four identical dipole magnets of length  $L_{d1}$ , deviation  $\theta_d$ , and separation  $L_{d1}$  between first and second dipole and  $L_{d2}$  between second and third dipole. It creates a linear strength  $r_{lc}$  given by  $r_{lc} = 2\theta_d^2(L_{d1} + 2L_{d2}/3)$ . The bunch can be easily lengthened for slippage handling by playing on the chicane strength according to  $\sigma_s^2 = \sigma_{s0}^2 + (r_{lc}\sigma_{\gamma 0}/\gamma)^2$ . Slice peak current drops as  $I_s = I_{s0}\sigma_{s0}/\sigma_s$ , but the slice energy spread is accordingly reduced as  $\sigma_{\gamma s} = \sigma_{\gamma 0}\sigma_{s0}/\sigma_s$  and electrons are sorted per slice in energy, as illustrated in figures 6(a) and (b). The chromatic emittance also drops. The bunch lengthening dramatically reduces all the downstream collective effects, as confirmed by additional simulations, including 3D space charge and coherent synchrotron radiation. Resistive wall and beam pipe geometry should also be considered. The slice energy spread of the beam is reduced from 1% to 0.1% with a bunch lengthened from 2 fs to 20 fs, leading to a large increase of the radiation peak power. Figure 6(c) shows full tracking through the transport, including expected FEL output power estimated with the 3D analytic model, together with GENESIS simulations. This figure shows that the longitudinal demixing manipulation enables the FEL power to grow significantly and to achieve efficient lasing, even in the 50–10 nm spectral range. The bunch length is increased from 4 up to 50 fs by the chicane, relaxing the slippage constraints. A good agreement is found between the analytic model and the GENESIS simulations, though somehow limited by the growth of several transverse modes. The chicane can be used

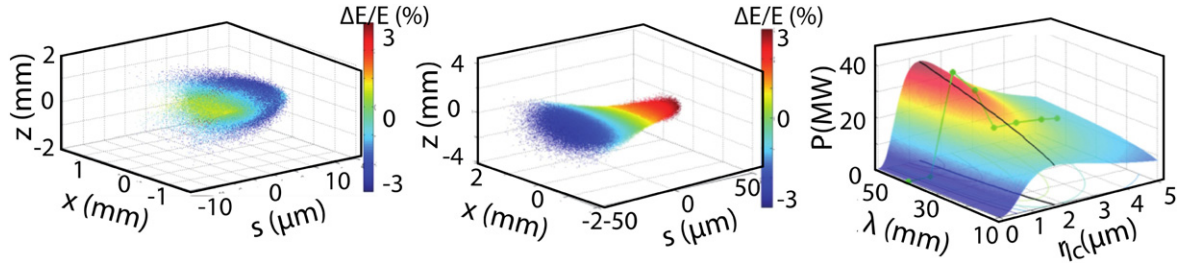


**Figure 6.** 3D plot of the electron bunch with color representation of the energy deviation: (a) before the chicane (2.2 kA, 4 fs RMS), (b) after the chicane (180 A, 40 fs RMS), and (c) FEL power (3D analytic expression and steady-state GENESIS) versus the chicane demixing strength. Same electrons’ beam parameters as for figure 5. FEL simulations with a U15 in-vacuum undulator of 1.5 T peak field.

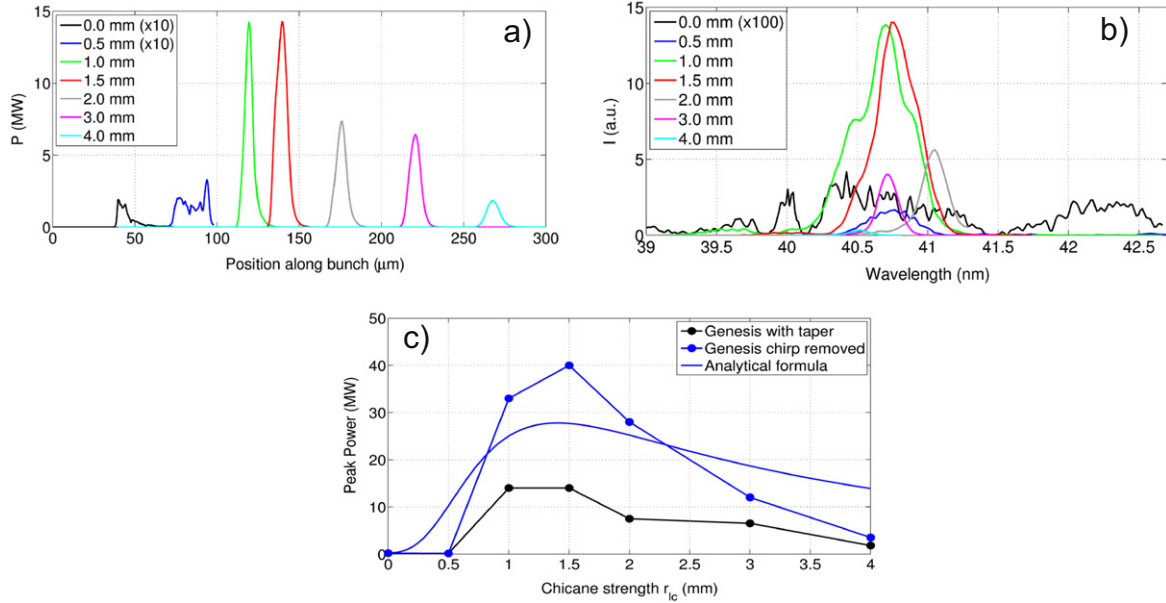


**Figure 7.** Time dependent GENESIS simulations (with and without chirp and taper): (a) temporal, (b) spectral FEL distributions, and (c) FEL power at 40 nm versus the chicane strength, with the parameters of figure 5. The spiky structure of the radiation disappears with increasing chicane strength.

as a knob to trade off between the energy spread reduction, the peak current decrease, and the slice emittance recovery, with a rather smooth optimum.

In fact, the chicane also introduces a linear energy chirp  $\gamma(s) = s/r_c$ , and the light pulse slips along the electronic distribution because of the speed difference so that the light falls out of resonance after several periods. In consequence, the magnetic field of the undulator is slightly changed along the propagation direction (the so-called taper) in order to maintain the resonance condition for its effective length. Further preliminary time-dependent GENESIS simulations considering the chirp and its compensation with the proper undulator taper [153–156] confirm the gain in peak power due to the chicane within 20% with respect to the analytic estimate (figure 7(a)). Figures 7(b) and (c) exhibit the spectral and temporal distributions of the achieved FEL considering the chirp and a taper compensation. They seem to indicate that, starting without chicane with a few fs long pulse with a broad and spiky spectrum, the FEL pulse is shaped by the chicane manipulation towards smooth Gaussian shapes, accompanied by a two orders of magnitude increase of peak power without

significant change of the FEL pulse duration (20–30 fs) in the single spike. It results in a gain of four orders of magnitude on the radiation brightness ( $10^{27}$  ph/s/mm<sup>2</sup>mrad<sup>2</sup>/0.1%BW at 40 nm).

Before entering the undulator, one has to refocus the electron bunch in the first part of the undulator. One can further take advantage of the particular correlation existing in the electron beam phase space, in adjusting smoothly the focusing of the electrons inside the undulator from slice to slice, by properly setting the first series of quadrupoles, the chicane, and an additional set of quadrupoles located before the undulator so that particles contribute more efficiently to the amplification. With this so-called ‘Chromatic-matching’ [152], the effective electron density is increased, and the peak FEL power is enhanced by one or two orders of magnitude.

Seeding is also largely considered for LWFA-based FEL. One can generate harmonics on crystals or in gas from the powerful laser which produces the electrons, with a natural synchronization with the electrons. Seeding will be quite beneficial for the LWFA-based FEL, since it will enable one to reduce the saturation length and to avoid a then too-large

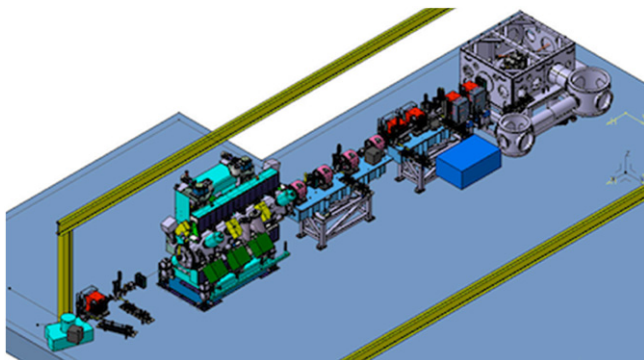


**Figure 8.** CATIA general integration view of the COXINEL LWFA demonstration setup. General view of the COXINEL LWFA demonstration setup (from right to left): LWFA chamber (gray) with the first set of quadrupoles and a current beam transformer, magnetic chicane (red), quadruplet of quadrupoles (pink), undulator (case of 2 meter U20 undulator), dipole for beam dump (red), and spectrometer (blue).

slippage. Furthermore, one can also aim at somehow playing with the FEL performance (such as spectral and temporal distributions, polarization, and up-frequency conversion).

In the frame of LUNEX5 studies, a test experiment is under preparation [159, 160]. Figure 8 shows the transport line from the LWFA electron source to the undulator. The FEL will use the electron beam generated at the Laboratoire d'Optique Appliquée (LOA) with the  $2 \times 60$  TW laser in the colliding scheme and the associated gas chamber, transport, and FEL equipment available or prepared at SOLEIL. This includes variable permanent magnet quadrupoles, FEL characterization tools, and available undulators from SOLEIL (one 2 m long in-vacuum undulator of 20 mm period U20, a 3 m long innovative cryo-ready in-vacuum U15 undulator [161]).

The alternative to the demixing chicane is to use a transverse gradient undulator [157, 158]. The concept here is to generate a linear horizontal dependence of the undulator vertical field combined with a dispersion of the electrons. The transverse gradient undulator is created by canting the magnets, resulting in  $\Delta K_u/K_u = \alpha x$ ,  $x$  being the horizontal coordinate. The dispersion function  $\eta$  links the transverse position with the energy variation according to  $x = \eta \Delta Y/Y$ . One can adjust the energy such as  $\eta = (2 + K_u^2)/\alpha K_u^2$ .

Further studies will include sensitivity to parameters and tolerance studies. The stability of LWFA can become challenging. From this prospect, the chicane setup might appear to be more robust than the transverse gradient one.

Additionally, start-to-end simulations starting from PIC calculations are under progress.

#### 4. Conclusion

Specific transverse and longitudinal manipulation of the electrons along the electron transport to the undulator to handle the LWFA electron beam properties towards FEL amplification have been discussed. The divergence can be

handled by strong quadrupoles located very close to the electron source. Electron beam manipulation by chicane decompression or by the use of transverse gradient undulator suggests that significant amplification with the present LWFA performance has become possible. The chicane 'sorts' the electrons by energy (in putting forward high energy particles and back low energy ones), reducing the slice energy spread and lengthening the bunch. Further, synchronized focusing, by taking advantage of the particular correlation existing in the electron beam phase space, can provide an efficient amplification. Seeding can also be applied, enabling one to reduce the undulator length and to somehow manipulate the FEL properties. In addition, the use of in-vacuum APPLE-II type undulators can be considered for polarization control.

An experimental demonstration would represent a major breakthrough, opening the way to the so-called fifth generation light source of compact laboratory-size FEL sources at reasonable cost. It would enable widespread use of these sources in a larger scale, revolutionizing access for researchers of different fields. Several groups are presenting working towards an experimental demonstration of the laser effect while exploring new concepts of electron beam manipulation with existing LWFA before stepping to a dedicated test machine. These expected results will then provide a major contribution towards the fifth generation light sources, with future compact light sources and FELs. Also, since LWFA appears to be an attractive candidate for the next generation of colliders, such an FEL experimental demonstration will provide an intermediate qualification in the goal towards TeV LWFA colliders of long-term interest for high energy physics.

#### Acknowledgments

M E Couprie and V Malka are grateful for support from the European Research Council for COXINEL (340015) and X-Five (339128) advanced grants.

#### References

- [1] Couprie M E and Filhol J M 2008 X radiation sources based on accelerators, synchrotron x-rays and condensed matter *C. R. Physique* **9** 487–506
- [2] Zholents A and Zolotarev M 1996 Femtosecond x-ray pulses of synchrotron radiation *Phys. Rev. Lett.* **76** 912
- [3] Deacon D A G and Madey J M J 1980 Isochronous storage-ring laser: a possible solution to the electron heating problem in recirculating free-electron lasers *Phys. Rev. Lett.* **44** 449–52
- [4] Wustefeld G *et al* 2011 *IPAC 2011 (Spain: San Sebastian)*  
Jankowiack A and Wustefeld G 2013 *Synch. Rad. News* 37–41
- [5] Madey J M J 1971 Stimulated emission of bremsstrahlung in a periodic magnetic field *Appl. Phys.* **42** 1906
- [6] Couprie M E and Valléau M 2012 Synchrotron radiation, polarisation, devices, new sources *Proc. 6th Int. School on 'Magnetism and Synchrotron Radiation: Towards the Fourth Generation Light Sources'* (Mittelwihr, France)

- Beaurepaire E, Bulou H, Joly L and Scheurer F (ed) 2013 *Proc. in Physics* vol 151 (Berlin: Springer) pp 51–94
- [7] Chapman H N *et al* 2011 *Nature* **470** 73–7
- [8] Tajima T and Dawson J M 1979 Laser electron accelerator *Phys. Rev. Lett.* **43** 267
- [9] Malka V *et al* 2011 Principle and applications of compact laser-plasma electron accelerator *Nature Phys.* **7** 219
- [10] Nakajima K 2008 Towards a table-top free-electron laser *Nature Phys.* **4** 92
- [11] Gruner F *et al* 2007 *Appl. Phys. B* **86** 431
- [12] Schlenvoigt H-P *et al* 2008 A compact synchrotron radiation source driven by a laser-plasma wakefield accelerator *Nature Phys.* **4** 130–3
- [13] Fuchs M *et al* 2009 Laser-driven soft-x-ray undulator source *Nature Phys.* **5** 826
- [14] Lambert G *et al* 2012 Progress on the generation of undulator radiation in the UV from a plasma-based electron beam *Proc. FEL Conf. (Nara, Japan)*
- [15] Colson W B 1981 The nonlinear wave equation for higher harmonics in free-electron lasers *IEEE J. Quantum Electron.* **17** 1417–27
- [16] Couprie M E and Filhol J M 2008 X radiation sources based on accelerators, synchrotron x-rays and condensed matter *C. R. Physique* **9** 487–506
- [17] Deacon D A G *et al* 1977 First operation of a free electron laser *Phys. Rev. Lett.* **38** 892–4
- [18] Billardon M, Elleaume P, Ortega J M, Bazin C, Bergher M, Velghe M, Petroff Y, Deacon D A G, Robinson K E and Mady J M J 1983 First operation of a storage-ring free-electron laser *Phys. Rev. Lett.* **51** 1652
- [19] Girard B, Lapiere Y, Ortega J M, Bazin C, Billardon M, Elleaume P, Bergher M, Velghe M and Petroff Y 1984 Optical frequency multiplication by an optical klystron *Phys. Rev. Lett.* **53** 2405
- [20] Prazeres R, Ortéga J M, Bazin C, Bergher M, Billardon M, Couprie M E, Fang H, Velghe M and Petroff Y 1987 First production of vacuum-ultraviolet coherent light by frequency multiplication in a relativistic electron beam *Europhys. Lett.* **4** 817–22
- [21] Prazeres R, Guyot-Sionnest P, Jaroszynski D, Ortéga J M, Billardon M, Couprie M E and Velghe M 1991 Coherent harmonic generation in VUV with the optical klystron on the storage ring Super-ACO *Nucl. Instrum. Methods Phys. Res. A* **304** 72–6
- [22] Kulipanov G N *et al* 1990 *Nucl. Instrum. Methods Phys. Res. A* **296** 1
- [23] Couprie M E, Garzella D, Delboulbé A, Velghe M and Billardon M 1993 Operation of the Super-ACO FEL in the UV range at 800 MeV *Europhys. Lett.* **21** 909–14
- [24] Yamada K, Yamazaki T, Sugiyama S, Ohgaki H, Noguchi T, Mikado T, Chiwaki M, Suzuki R and Tomimasu T 1993 FEL oscillation on TERAS *Nucl. Instrum. Methods Phys. Res. A* **331** 103–6
- [25] Yamazaki T *et al* 1993 First lasing of the NIJI-IV storage-ring free-electron laser *Nucl. Instrum. Methods Phys. Res. A* **331** 27–33
- [26] Hama H, Yamazaki J and Isoyama G 1994 *Nucl. Instrum. Methods Phys. Res. A* **341** 12
- [27] Nölle D, Garzella D, Geisler A, Gianessi L, Hirsch M, Quick H, Ridder M, Schmidt T and Wille K 2000 First lasing of the FELICITA I FEL at DELTA *Nucl. Instrum. Methods Phys. Res. A* **445** 128–33
- [28] Litvinenko V N, Park S H, Pinayev I V, Wu Y, Emamian M, Hower N, Morcombe P, Oakeley O, Swift G and Wang P 1999 OK-4/Duke storage ring FEL lasing in the deep-UV *Nucl. Instrum. Methods Phys. Res. A* **429** 151–8
- [29] Marsi M *et al* 2002 Operation and performance of a free electron laser oscillator down to 190 nm *Appl. Phys. Lett.* **80** 2851–3
- Trovo M *et al* 2002 Operation of the European storage ring FEL at ELETTRA down to 190 nm *Nucl. Instrum. Methods Phys. Res. A* **483** 157–61
- [30] Tomimasu T *et al* 1996 The FELI FEL facilities—challenges at simultaneous FEL beam sharing systems and UV-range FELs *Nucl. Instrum. Methods Phys. Res. A* **375** 626–31
- [31] Neil G R *et al* 2006 Jefferson lab: the JLab high power ERL light source *Nucl. Instrum. Methods Phys. Res. A* **557** 9–15
- [32] Minehara E J, Sugimoto M, Sawamura M, Nagai R, Kikuzawa N, Yamanouchi T and Nishimori N 1999 A 0.1 kW operation of the JAERI superconducting RF LINAC-based FEL *Nucl. Instrum. Methods Phys. Res. A* **429** 9–11
- [33] Couprie M E, Billardon M, Velghe M and Prazeres R 1991 Study of the transverse modes of the Super-ACO FEL *Nucl. Instrum. Methods Phys. Res. A* **304** 53–7
- [34] Couprie M E, Tauc P, Merola F, Delboulbé A, Garzella D, Hara T and Billardon M 1994 Fluorescence decays and rotational dynamics of the NADH coenzyme, first use of the UV Super-ACO free electron laser *Rev. Sci. Instrum.* **65** 1495
- [35] Marsi M, Couprie M E, Nahon L, Garzella D, Delboulbé A, Hara T, Bakker R, Indlekofer G, Billardon M and Taleb-Ibrahimi A 1997 Surface states and space charge layer dynamics on Si(111)2×1: a free electron laser-synchrotron radiation study *Appl. Phys. Lett.* **70** 895–7
- [36] Edwards G S *et al* 2003 Free-electron-laser-based biophysical and biomedical instrumentation *Rev. Sci. Instrum.* **74** 3207–45
- [37] Weller H R and Ahmed M W 2003 The HIγS facility: a free-electron laser generated gamma-ray beam for research in nuclear physics *Mod. Phys. Lett. A* **18** 1569
- [38] Neil G R, Jefferson Lab FEL Team 1998 Industrial applications of the Jefferson Lab high-power free-electron laser *Nucl. Instrum. Methods Phys. Res. B* **144** 40–9
- [39] Marsi M, Trovo M *et al* 2002 Operation and performance of a free electron laser oscillator down to 190 nm *Appl. Phys. Lett.* **80** 2851–3
- [40] Couprie M E, Billardon M, Bazin C, Bergher M, Fang H, Ortéga J M, Prazeres R, Velghe M and Petroff Y 1988 Optical properties of multilayer mirrors exposed to synchrotron radiation *Nucl. Instrum. Methods Phys. Res. A* **272** 166–73
- [41] Garzella D, Couprie M E, Hara T, Nahon L, Brazuna M, Delboulbé A and Billardon M 1995 Mirror degradation and heating in storage ring free electron lasers *Nucl. Instrum. Methods Phys. Res. A* **358** 387
- [42] Gatto A *et al* 2002 Multiscale degradations on FEL optics *Nucl. Instrum. Methods Phys. Res. A* **483** 172–6
- [43] Bonifacio R, Pellegrini C and Narducci L M 1984 Collective instabilities and high gain regime in a free electron laser *Optics Comm.* **50** 373–8
- [44] Kim K J 1986 Tree dimensional analysis of coherent amplification and self amplified spontaneous emission in free electron laser *Phys. Rev. Lett.* **57** 1871–4
- [45] Kondratenko A M and Saldin E L 1980 *Part. Accelerators* **10** 207
- [46] Kim K J and Xie M 1993 *Nucl. Instrum. Methods Phys. Res. A* **331** 359
- [47] Xie M 1995 *Proc. of the PAC'95 Conf. (Trieste, Italy)* vol 1 p 183
- [48] Milton S V *et al* 2001 Exponential gain and saturation of a self-amplified spontaneous emission free-electron laser *Science* **292** 2037
- [49] Ackermann W *et al* 2007 Operation of a FEL from the extreme UV to the water window *Nat. Photonics* **1** 336–42
- [50] Honkavaara K, Faatz B, Feldhaus J, Schreiber S, Treusch R and Vogt M 2014 Flash: first soft x-ray FEL

- operating two undulator beamlines simultaneously *Proc. FEL Conf. (Basel, Switzerland) JACoW* to appear
- [51] Shintake *et al* 2008 A compact FEL for generating coherent radiation in the extreme ultraviolet region *Nat. Photonics* **2** 555–9
- [52] Emma P *et al* 2010 First lasing and operation of an Angstrom-wavelength free-electron laser *Nat. Photonics* **4** 641
- [53] Huang Z *et al* 2010 *Phys. Rev. ST Accel. Beams* **13** 020703
- [54] Raubenheimer T 2014 The LCLS-II, a new FEL facility at SLAC *Proc. FEL Conf. (Basel, Switzerland) JACoW* to appear
- [55] Ishikawa T *et al* 2012 A compact x-ray free-electron laser emitting in the sub-ångström region *Nat. Photonics* **6** 540–4
- [56] Townes C 2003 *A Century of Nature, 21 Discoveries that Changed Science in the World* (Chicago, IL: University of Chicago Press)
- [57] Seibert M M *et al* 2011 *Nature* **470** 78–81
- [58] Kirian R A *et al* 2011 *Acta Crystallography A* **67** 131–40
- [59] Young L *et al* 2010 *Nature* **466** 56
- [60] Berrah N *et al* 2010 *J. Modern Opt.* **57** 1015
- [61] Doumy G *et al* 2011 *Phys. Rev. Lett.* **106** 083002
- [62] Richter M *et al* 2010 *J. Phys. B: At. Mol. Opt. Phys.* **43** 194005
- [63] Meyer M, Costello J T, Düsterer S, Li W B and Radcliffe P 2010 *J. Phys. B: At. Mol. Opt. Phys.* **43** 194006
- [64] Glownia J M *et al* *Opt. Express* **18** 017620
- [65] Galtier E *et al* 2011 *Phys. Rev. Lett.* **106** 164801
- [66] Yoon M *et al* 2004 The European x-ray laser project XFEL, TDR Proc. FEL04, JACoW July 2006 ([www.xfel.desy.de](http://www.xfel.desy.de)) pp 183–6
- [67] Yoon M *et al* 2004 *Proc. FEL04, JACoW* pp 183–6
- [68] Ganter R *et al* 2010 *Swiss FEL Conceptual Design Report* ([www.psi.ch/swissfel/HomeEN/SwissFEL\\_CDR\\_web\\_small.pdf](http://www.psi.ch/swissfel/HomeEN/SwissFEL_CDR_web_small.pdf))
- [69] Saldin E *et al* 1998 *Opt. Commun.* **148** 383–403
- [70] Yu L H and Ben Z I 1997 High-gain harmonic generation of soft x-rays with the ‘fresh bunch’ technique *Nucl. Instrum. Methods Phys. Res. A* **393** 96
- [71] McPherson A, Gibson G, Jara H, Johann U, Luk T S, McIntyre I A, Boyer K and Rhodes C K 1987 Studies of multiphoton production of vacuum ultraviolet radiation in the rare gases *J. Opt. Soc. Am. B* **4** 595
- [72] Ferray M, L’Huillier A, Li X F A, Lompre L A, Mainfray G and Manus C 1988 Multiple-harmonic conversion of 1064 nm radiation in rare gases *J. Phys. B: At. Mol. Opt. Phys.* **21** L31
- [73] Yu L-H *et al* 2000 High-gain harmonic-generation free-electron laser *Science* **289** 932
- [74] Giannessi L, Musumeci P and Spampinati S 2005 Nonlinear pulse evolution in seeded free-electron laser amplifiers and in free-electron laser cascades *J. Appl. Phys.* **98** 043110
- [75] Lambert G *et al* Injection of harmonics generated in gas in a free-electron laser providing intense and coherent extreme ultraviolet light *Nat. Phys.* **4** 296–30
- [76] Takahashi E J 2011 Extreme ultraviolet free electron laser seeded with high-order harmonic of Ti:sapphire laser *Optics Express* **1** 317–24
- [77] Labat M *et al* 2011 High-gain harmonic-generation free-electron laser seeded by harmonics generated in gas *Phys. Rev. Lett.* **107** 224801
- [78] Lechner C *et al* 2012 *Proc. FEL 2012 (Nara, Japan, 2012)*
- [79] Llaría E *et al* 2012 Tunability experiments at the FERMI@Elettra free-electron laser *New J. Phys.* **14** 113009
- [80] Yu L H *et al* 2002 *Nucl. Instrum. Methods Phys. Res. A* **483** 493
- [81] Giannessi L 2014 Pulse control in FEL amplifier *Proc. FEL Conf. (Basel, Switzerland, 2014)*
- [82] Sasaki S *et al* 1992 *Jpn. J. Appl. Phys.* **31** L194
- [83] Lambert G, Hara T, Labat M, Tanikawa T, Tanaka Y, Yabashi M, Garzella D, Carré B and Couprie M E 2009 Seed level requirement for improving the temporal coherence of a free electron laser *Europhys. Lett.* **88** 54002
- [84] Tanikawa T, Lambert G, Hara T, Labat M, Tanaka Y, Yabashi M, Chubar O and Couprie M E 2011 Nonlinear harmonic generation in a free-electron laser seeded with high harmonic from gas *Europhys. Lett.* **3** 34001
- [85] Stupakov G 2009 Echo-enabled harmonic generation free-electron laser *Phys. Rev. Lett.* **102** 074801
- [86] Xiang D *et al* 2010 Demonstration of the echo-enabled harmonic generation technique for short-wavelength seeded free electron lasers *Phys. Rev. Lett.* **105** 114801
- [87] Hemsing E, Dunning M, Hast C, Raubenheimer T O, Weathersby S and Xiang D 2014 Highly coherent vacuum ultraviolet radiation at the 15th harmonic with echo-enabled harmonic generation technique *Phys. Rev. ST Accel. Beams* **17** 070702
- [88] Zhao Z T *et al* 2012 First lasing of an echo-enabled harmonic generation free-electron laser *Nat. Photonics* **6** 360–3
- [89] Xiang D and Stupakov G 2011 Triple modulator chicane scheme for seeding sub-nanometer x-ray free-electron lasers *New J. Phys.* **13** 093028
- [90] Reiche S *et al* 2008 *Nucl. Instrum. Methods Phys. Res. A* **593** 45–8
- [91] Din Y *et al* 2009 *Phys. Rev. Lett.* **102** 254801
- [92] Giannessi L *et al* 2011 *Phys. Rev. Lett.* **106** 144801
- [93] McNeil B 2014 Review of coherent SASE schemes *Proc. FEL JACoW (Basel, Switzerland)*
- [94] Feldhaus J, Saldin E L, Schneider J R, Schneidmiller E A and Yurkov M V 1997 Possible application of x-ray optical elements for reducing the spectral bandwidth of an x-ray SASE FEL *Opt. Commun.* **140** 341
- [95] Geloni G L 2011 A novel self-seeding scheme for hard x-ray FELs *J. Modern Optics* **58** 1391–403
- [96] Amann J *et al* 2012 Demonstration of self-seeding in a hard-x-ray free-electron laser *Nat. Photonics* **6** 693–8
- [97] Inagaki T *et al* 2014 Hard x-ray self-seeding set-up and results at SACLA *Proc. FEL Conf. (Basel, Switzerland)*
- [98] Singer A *et al* 2008 *Phys. Rev. Lett.* **101** 254801
- [99] Bachelard R *et al* 2011 Single-shot wavefront analysis of SASE harmonics in different FEL regimes *Phys. Rev. Lett.* **106** 234801
- [100] Prazeres R, Glotin F, Insa C, Jaroszynski D A and Ortega J M 1998 Two colour operation of a free electron laser and applications in the mid-infrared *Nucl. Instrum. Methods Phys. Res. A* **407** 464
- [101] Prazeres R, Glotin F, Insa C, Jaroszynski D A and Ortega J M 1998 Two colour operation of a Free Electron Laser and applications in the mid-infrared *Eur. Phys. J. D* **3** 87
- [102] Lutman A A *et al* 2013 Experimental demonstration of fs two-color x-ray FELs *Phys. Rev. Lett.* **110** 134801
- [103] Labat M, Joly N, Bielawski S, Swaj C, Bruni C and Couprie M E 2009 Pulse splitting in short wavelength free electron laser *Phys. Rev. Lett.* **103** 264801
- [104] De Ninno G *et al* 2013 *Phys. Rev. Lett.* **110** 064801
- [105] Corlett J N *et al* 2011 A next generation light source facility at LBNL 2011 *Particle Accelerator Conf. PAC 11 (New York, 2011)*
- [106] Hara T *et al* 2013 *Phys. Rev. ST Accel. Beams* **16** 080701
- [107] Naranjo B, Valloni A, Putterman S and Rosenzweig J B 2012 Stable charge-particle acceleration and focusing in a laser accelerator using spatial harmonics *Phys. Rev. Lett.* **109** 176803
- [108] Rosenzweig J B *et al* 2012 The GALAXIE all-optical FEL project *AIP Conf. Proc.* **1507** 493
- [109] Kimura W *et al* 2004 *Phys. Rev. Lett.* **92** 154801
- [110] Musumeci P *et al* 2005 *Phys. Rev. Lett.* **94** 154801
- Musumeci P 2013 *European Advanced Accelerator Concepts Workshop (EAAC) Elba*

- [111] Couprie M E *et al* 2012 *The LUNEX5 project in France J. Phys.: Conf. Ser.* **425** 072001
- [112] LUNEX5 Conceptual Design Report ([www.lunex5.com/spip.php?article33](http://www.lunex5.com/spip.php?article33))
- [113] Esarey E, Schroeder C B and Leemans W P 2009 *Rev. Mod. Phys.* **81** 1229
- [114] Malka V 2012 *Phys. Plasmas* **19** 055501
- [115] Malka V *et al* 2002 *Science* **22** 298
- [116] Faure J, Rechatin C, Norlin A, Lifschitz A, Glinec Y and Malka V 2006 *Nature* **444** 05393
- [117] Bulanov S, Naumova N, Pegoraro F and Sakai J 1998 *Phys. Rev. E* **58** R5257
- [118] Geddes C G R *et al* 2008 *Phys. Rev. Lett.* **100** 215004
- [119] Kim U, Hafz N and Suk H 2004 *Phys. Rev. E* **69** 026409
- [120] Chien T-Y, Chang C-L, Lee C-H, Lin J-Y, Wang J and Chen S-Y 2005 *Phys. Rev. Lett.* **94** 115003
- [121] Tomassini P *et al* 2003 *Phys. Rev. ST Accel. Beams* **6** 121301
- [122] Faure J, Rechatin C, Lundh O, Ammoura L and Malka V 2010 *Phys. Plasmas* **17** 083107
- [123] Brantov A V *et al* 2008 *Phys. Plasmas* **15** 073111
- [124] Gonsalves A J *et al* 2011 *Nat. Phys.* **7** 862
- [125] Koyama K *et al* 2009 *Nucl. Instrum. Methods Phys. Res. A* **608** S51
- [126] Schmid K *et al* 2010 *Phys. Rev. ST Accel. Beams* **13** 091301
- [127] Rechatin C, Faure J, Ben-Ismaïl A, Lim J, Fitour R, Specka A, Videau H, Tafzi A, Burgy F and Malka V 2009 Controlling the phase-space volume of injected electrons in a laser-plasma accelerator 2009 *Phys. Rev. Lett.* **102** 164801
- [128] Davoine X, Lefebvre E, Rechatin C, Faure J and Malka V 2009 *Phys. Rev. Lett.* **102** 065001
- [129] Lehe R, Lifschitz A F, Davoine X, Thauray C and Malka V 2013 *Phys. Rev. Lett.* **111** 085005
- [130] Mangles S *et al* 2004 *Nature* **431** 535
- [131] Faure J *et al* 2004 *Nature* **431** 541
- [132] Geddes C G R *et al* 2004 *Nature* **431** 538
- [133] Leemans W P, Nagler B, Gonsalves A J, Toth C, Nakamura K, Geddes C G R, Esarey E, Schroeder C B and Hooker S M 2006 GeV electron beams from a centimetre-scale accelerator *Nature Phys.* **2** 696  
Faure J *et al* 2006 *Nature* **444** 737
- [134] Malka V *et al* 2008 *Nat. Phys.* **4** 447–53
- [135] Fritzler S *et al* 2004 *Phys. Rev. Lett.* **92** 165006
- [136] Sears C M S *et al* 2010 *Phys. Rev. ST Accel. Beams* **13** 092803
- [137] Brunetti E *et al* 2010 *Phys. Rev. Lett.* **105** 215007
- [138] Leemans W *et al* 2009 *Phys. Today* **62** 44
- [139] Fawley W M *et al* 2006 *Proc. FEL06 (Berlin, Germany)* pp 455–8
- [140] Anania M P *et al* 2010 The ALPHA-X beam line: towards a compact FEL *Proc. IPAC10 (Kyoto, Japan, 2010)* pp 2263–5
- [141] [www.mpg.de/APS/gruener.php](http://www.mpg.de/APS/gruener.php)
- [142] Couprie M E *et al* 2014 The status of the LUNEX5 project *Proc. FEL'14 (Basel, Switzerland, 2014)*
- [143] Anticiet P *et al* 2012 *J. Appl. Phys.* **112** 044902
- [144] Migliorati M *et al* 2013 *Phys. Rev. Spec. Topics AB* **16** 011302
- [145] Couprie M E 2012 *The LUNEX5 project, Future Light Source meeting (oral presentation, Jefferson Lab, March 2012)*
- [146] Anania M P *et al* 2009 *Proc. of SPIE Conf.* **7359** 735916
- [147] Halbach K 1981 *Nucl. Instrum. Methods Phys. Res.* **187** 109–17
- [148] Xie M 1995 *Proc. PAC95 (Trieste, Italy)* **1** p 183
- [149] Reiche S 1999 *Nucl. Instrum. Methods Phys. Res. A* **429** 243
- [150] Maier A R *et al* 2012 Demonstration scheme for a laser-plasma-driven free-electron laser 2012 *Phys. Rev. X* **2** 031019
- [151] Schroeder C B *et al* 2012 *Proc. FEL Conf. (Nara, Japan, 2012)*
- [152] Loulergue A 2013 *ICFA-sponsored workshop series on Physics and Applications of High Brightness Beams (San Juan, Puerto Rico, 25–28 March)* (<http://pbpl.physics.ucla.edu/HBEB2013/index.html>)
- [153] Kroll N M *et al* 1980 *Phys. Quant. Elect.* **7** 113
- [154] Bonifacio R *et al* 1990 *Nuovo Cimento* **13** 1
- [155] Giannessi L *et al* 2011 *Phys. Rev. Lett.* **106** 144801
- [156] Reiche S 1999 *Nucl. Instrum. Methods Phys. Res. A* **429** 243
- [157] Huang Z *et al* 2012 Compact x-ray free-electron laser from a laser-plasma accelerator using a transverse-gradient undulator *Phys. Rev. Lett.* **109** 204801
- [158] Smith T *et al* 1979 *J. Appl. Phys.* **50** 4580
- [159] Couprie M E *et al* 2014 Experiment preparation towards a demonstration of laser plasma based free electron laser amplification *Proc. FEL'14 (Basel, Switzerland, 2014)*
- [160] Labat M, Hubert N, El Ajjouri M, Cassinari L, Bourrassin-Bouchet C, Loulergue A and Couprie M E 2014 Electron beam diagnostics for COXINEL *Proc. FEL'14 (Basel, Switzerland, 2014)*
- [161] Benabderrahmane C *et al* 2012 *Nucl. Instrum. Methods Phys. Res. A* **669** 1–6